INFLUENCE OF NANOPARTICLE'S SIZE ON MICROSTRUCTURE OF OXIDE COATINGS

J. KORZEKWA [1], *A. GĄDEK-MOSZCZAK* [2], *M. ZUBKO* [3]

[1] *Institute of Technology and Mechatronics, University of Silesia, Sosnowiec, Poland;*
[2] *Institute of Applied Informatics, Krakow University of Technology, Poland;*
[3] *Institute of Materials Science, University of Silesia, Chorzow, Poland*

The microstructure and structure of composite coatings prepared on aluminum substrates are studied. Amorphous oxide layers Al_2O_3 are obtained on EN AW 5251 aluminum alloy. In the Al_2O_3 coating two kinds of inorganic fullerene-like (IF) tungsten disulfide (WS_2) nanoparticles (NPs) are introduced by a dip coating method. In order to show the difference in the possibility of introducing the NPs in the microstructure of Al_2O_3 the scanning electron microscopy and transmission electron microscopy analysis are carried out. Image processing and analysis were conducted in order to study the shape and size of the IF-WS_2 nanoparticles. Visual comparative analysis shows the difference of nanopowders quality that greatly affects their ability to form agglomerates, and, hence, strongly influences the possibility of introducing the NPs into nanopores.

Keywords: *composite coatings, nanolubricants, image processing, shape of nanoparticles, size of nanoparticles.*

Inorganic fullerene-like (IF) tungsten disulfide (WS_2) nanoparticles (NPs) are one of the most commonly used nanolubricant. Dependence of the friction mechanism of IF-WS_2 NPs, like exfoliation, rolling and sliding on the normal stress has been study by Tevet et al. [1]. The mechanism of WS_2 NPs behavior in high-pressure contacts was presented by Ratoi et al. [2]. It is generally accepted that that agglomeration has strong influence on nanoparticles properties [3–5]. Much research in recent years has been focused on technical barriers for scaling up the IF-WS_2 which lie in the powder agglomeration and superficial reaction [6, 7]. Usually agglomerates limit or reduce the role of nanoparticles. Therefore it is necessary to know the shape and size of nanoparticles which are used in various applications [8].

Escobar et al. [9] filled the pores of the nanoporous aluminum oxide substrate with polytetrafluoroethylene (PTFE) particles, applying the sedimentation technique. The 200 nm sized PTFE particles were noticed only on the top of the surface and blocked the entrance to the pores. The smaller PTFE particles with a diameter of 90 nm were able to enter to the deeper part of the structure of anodic film. The insertion of the particles inside the anodic film was explained by the phenomena of surface tension [10] and capillary forces [11, 12]. Hu et al. [13] introduced C_{60} particles into the anodic oxide matrix, using the immersion method, emphasizing how important it is to enlarge pores of anodic oxide before self-lubricating treatment. In previous research the authors [14] showed that aluminum-oxide film could be loaded with nanoparticles of IF-WS_2, which were obtained in laboratory condition. It is well known that knowledge about the shape and size of the nanolubricant play a major role in technological process. Despite the breadth of research concerning different kinds of nanopowders introduced into anodic oxide layers, as for as we know, little research has been published regarding the influence of IF-WS_2 nanoparticle size and shape on microstructure of aluminum oxide layer.

Corresponding author: J. KORZEKWA, e-mail: joanna.korzekwa@us.edu.pl

The present article shows the differences between possibilities of introducing two kinds of IF-WS_2 NPs to the anodic oxide layer. First kind of nanoparticles was obtained in laboratory conditions [6]; the second one was commercially available product (NanoMaterials Ltd). To this purpose microstructural analysis using scanning electron microscopy (SEM), transmission electron microscopy (TEM) techniques, image processing and analysis carried on Aphelion 4.2 software were conducted.

Materials and methods. ***Sample preparation.*** Aluminum oxide Al_2O layers with IF-WS_2 coating were fabricated on EN AW 5251 aluminum alloy surface according to a two-steps method. Firstly, the film was obtained by the electro-oxidation of the aluminum alloy in a ternary solution consisting of sulfuric, oxalic and phthalic acids. In the second step of the process the IF-WS_2 NP were introduced into the porous alumina film by the dip coating method. The details of this method are described by Korzekwa et al. [14]. Two kinds of IF-WS_2 nanoparticles were used in the presented studies. First kind of NPs was obtained in laboratory condition [6] (designated as NPs-1 in this paper). Second one was commercially available IF-WS_2 nanoparticles from NanoMaterials Ltd (designated as NPs-2 in this paper). The NPs of IF-WS_2 were dispersed in 35 vol.% ethanol (C_2H_6O)/water mixture. The aluminum sheets were dip coted in the mixture and placed in the ultrasonic bath in order to facilitate the introduction of the NPs in the nanopores of Al_2O_3 coating. The surfaces of samples after tribological tests were used for SEM and computer image analysis. Tribological test was performed on a T17 tester, a pin-on-plate in a reciprocating motion, at room temperature, at a humidity of 30±5%, using 0.5 MPa pressure at an average sliding speed of 0.2 m/s in dry friction conditions. The tribological test was conducted at a sliding distance of 15 km. The commercial TG15 plastic pin of a diameter of 9 mm was used as a counter-body [15].

Micro- and nanostructural characterization. Microanalyses of surface, fresh cross-section and polished cross-section of Al_2O_3 with IF-WS_2 coatings were studied by a HITACHI S-4700 scanning electron microscope (SEM) with NORAN Vantage digital energy dispersive X-ray microanalysis (EDS) system.

Transmission electron microscopy (TEM) micrographs of the studied nanoparticles were recorded on a high resolution (HRTEM) JEOL 3010 microscope working at 300 kV equipped with 2 k×2 k Orius^{TM} 833 SC200D Gatan CCD camera.

Analysis of the nanoparticles shape and size. Image processing and analysis were conducted using Aphelion 4.2 software. Preprocessing stage was limited to a standard image quality improvement by filtering and reducing noise effect. In order to proper assess the numbers of the particles and its shape the cluster split transformation has been done. In particular cases manual correction of the obtained result was needed. Particles area, shape factors and diameters were determinate. The area is measured as a sum of all pixels building each of particles on the binary images, corrected by the scale factor. For shape description several parameters were used, namely: Crofton perimeter (P_C), MBR_High, MBR_Width, elongation factor (E) and circularity (C).

Crofton perimeter is calculated using Crofton formula [16]. It is the best approximation of the perimeter of the particles in the discrete space. To assess of the Crofton perimeter is necessary to determine the value of the circularity shape factor. Circularity is calculated using the formula:

$$C = \frac{4\pi \cdot A}{P_C^2}.$$

For circle circularity the value of factor is equal to 1.

MBR_Hight is the length of the smallest side of the minimum bounding rectangle of detected grain (Fig. 1). MBR_Width is the length of the largest side of the minimum bounding rectangle.

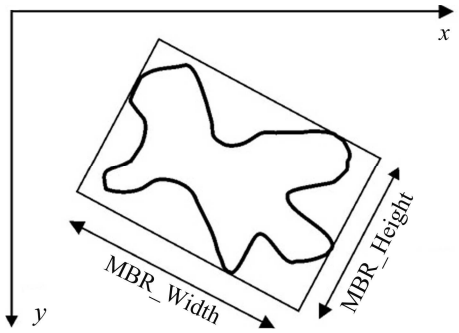

Fig. 1. Scheme of the MBR_Width and MBR_Height parameters indication.

Elongation factor is calculated as a ratio of the MBR_Heigh and MBR_Width value:

$$E = \frac{\text{MBR\_Height}}{\text{MBR\_Width}}.$$

This shape factor is sensitive to the elongation of the objects, regardless of the particles orientation in the coordinate system. The value of elongation equal 1, means that the analyzed shape is close to the circle or square.

Results and discussion. After technological process the samples of Al_2O_3/IF-WS_2 were analyzed by the SEM technique. Microstructures of the surface and fresh-cross section of Al_2O_3/IF-WS_2 coating with NPs-1 are presented in Fig. 2, respectively. The nanoparticles were introduced into nanopores according to the sedimentation technique. As it was shown in Fig. 2*a* it was possible to insert the fine grains of NPs-1 in the nanopores and according to the force of gravity the NPs-1 shifted to the deeper part of Al_2O_3 coating.

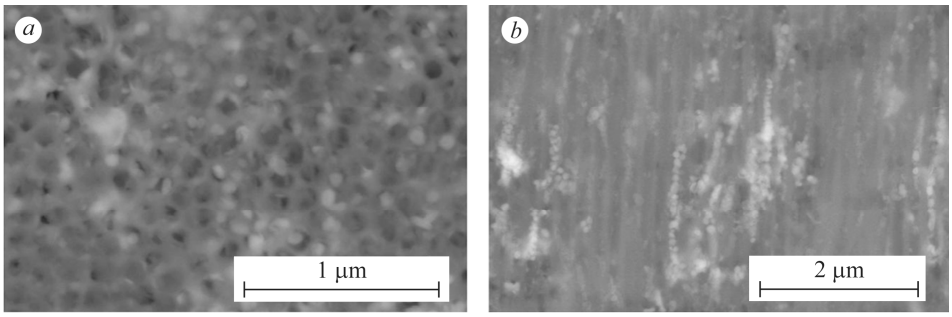

Fig. 2. Microstructure of the surface (*a*) and fresh-cross section (*b*) of Al_2O_3/IF-WS_2 coating with NPs-1.

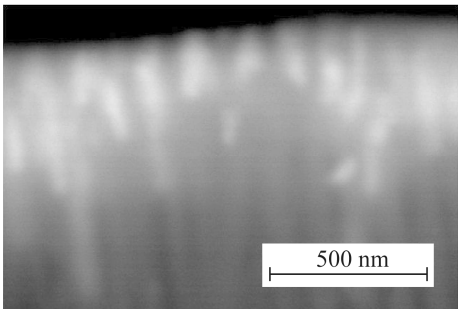

Fig. 3. Microstructure of polished cross-section of Al_2O_3/IF-WS_2 coating with NPs-2 after tribological test.

Similar analysis was carried out for Al_2O_3/IF-WS_2 coating with NPs-2. However the NPs-2 was visible in the nanopores only after tribological test. The NPs-2 was not observed in the material pores after sedimentation technique. In Fig. 3 presents the polished cross-section of Al_2O_3/IF-WS_2 coating with NPs-2 after tribological test. The NPs-2 was visible very closely to the surface of Al_2O_3 coatings. This analysis has suggested that the NPs-2 were on the Al_2O_3 surface and during sliding contact it has been introduced into nanopores as a result of load force between coating and the counter – body. This fact pointed out that there is probably a difference in shape and size between NPs-1 and NPs-2 which influence the methods of introducing the NPs to the structure of Al_2O_3.

In order to confirm the above suppose the TEM analysis of NPs-1 and NPs-2 was performed. TEM images of NPs-1 and NPs-2 are shown respectively (Fig. 4).

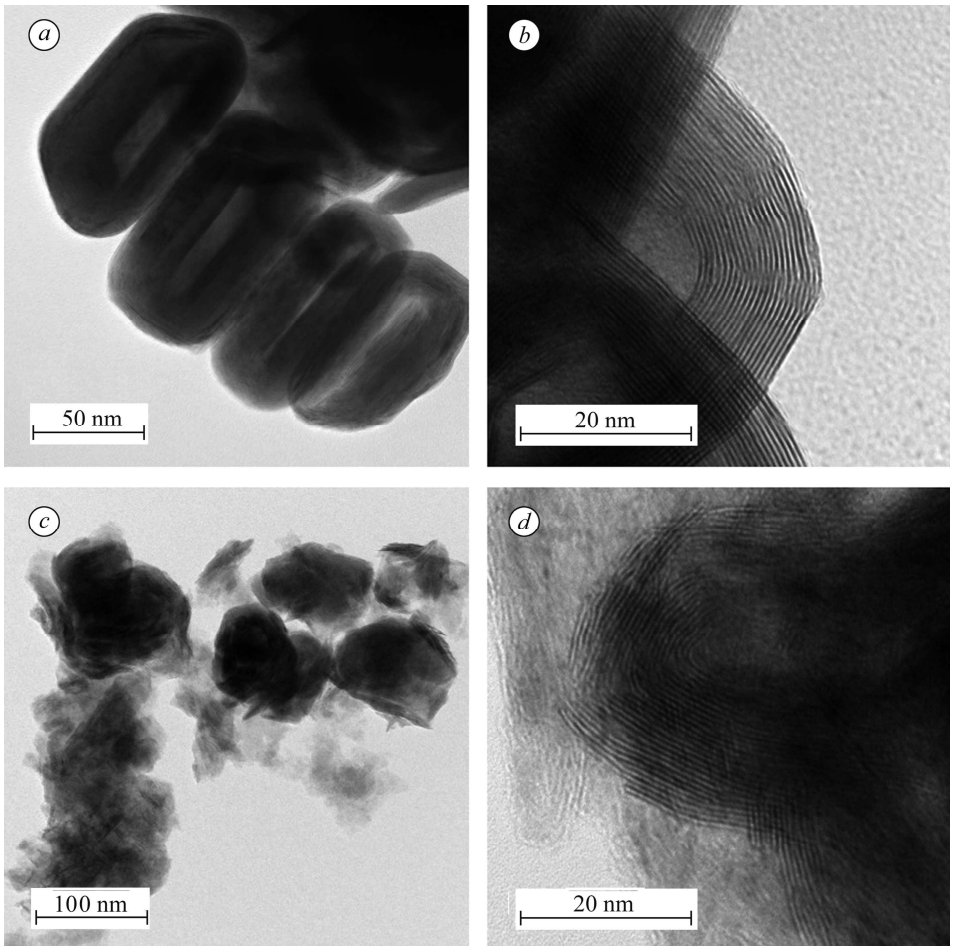

Fig. 4. TEM bright field (*a*) and high resolution (*b*) image of NPs-1 nanoparticles and TEM bright field (*c*) and high resolution (*d*) image of NPs-2 nanoparticles.

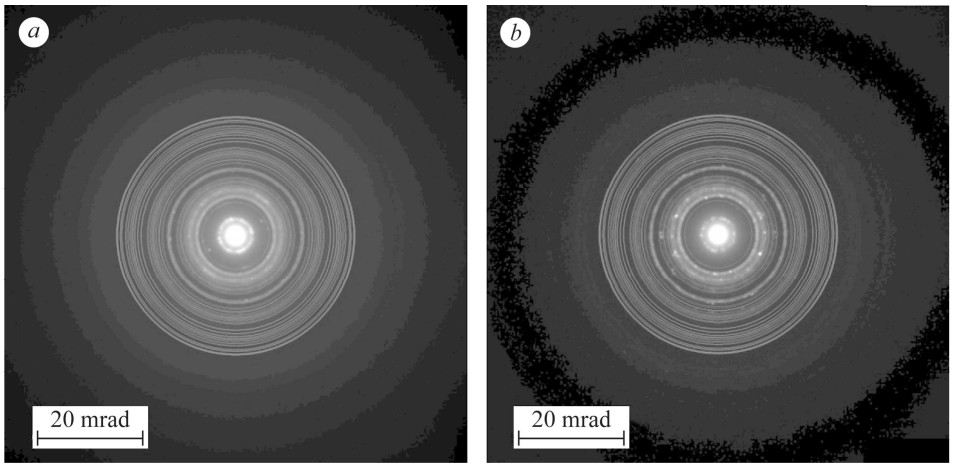

Fig. 5. The selected area electron diffraction patterns of: (*a*) NPs-1 recorded from the area shown in Fig. 3*a* and (*b*) NPs-2 recorded from the area shown in Fig. 4*a*. White circles correspond to the theoretical positions of diffraction rings for WS_2 structure taken from Crystallography Open Data Base ref cod 9012192.

In Fig. 4*a*, *b* NPs-1 nanosized grains with regular shape and clearly defined edges are visible. For NPs-2 unformed structure of grains with jagged and fuzzy contours are mostly observed (Fig. 4*c*, *d*). The NPs-2 additionally formed agglomerates. However as seen in the high resolution images (Fig. 4*b*, *d*), both materials possess the expected layered structure. In both cases the EDS analysis confirmed that the NPs-1 and NPs-2 have the same chemical composition (see Table 1). Based on the recorded selected area the electron diffraction patterns (Fig. 5) it is visible that NPs-1 and NPs-2 have the same crystal structure of WS_2 (Fig. 6).

Table 1. The results of the EDS analysis of NPs-1 and NPs-2

Element	NPs-1		NPs-2	
	wt.%	at.%	wt.%	at.%
S (K-line)	26.6	67.5	26.2	67.1
W (M-line)	73.4	32.5	73.8	32.9
Total	100.00	100.00	100.00	100.00

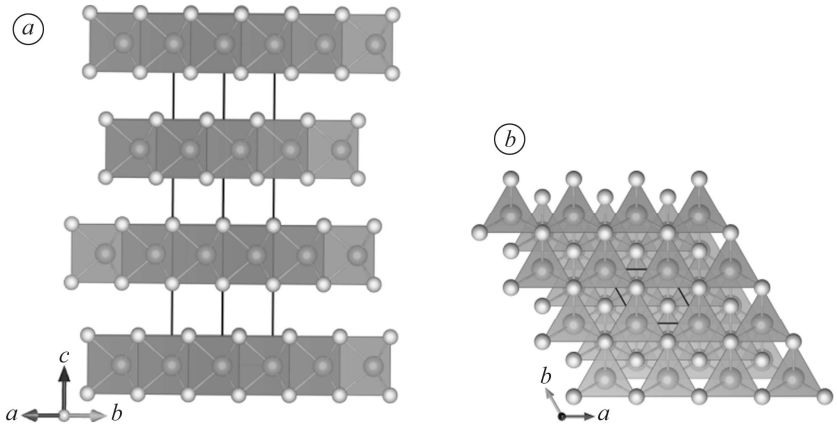

Fig. 6. Crystal structure of hexagonal WS_2: *a* – projection along [110] direction; *b* – along [001] direction.

Table 2 gives the measurements of area, Crofton Perimeter, MBR_Hight and MBR_Width, elongation and circularity of NPs-1 and NPs-2.

Table 2. Size and shape parameters of NPs-1 and NPs-2 grains

Parameter	moments	NPs-1	NPs-2
Area, nm^2	mean	8214.09	9724.46
	st. dev	5985.20	7202.20
Crofton perimeter, nm	mean	413.96	508.87
	st. dev	272.25	260.92
MBR_Height, nm	mean	85.20	96.06
	st. dev	36.43	40.35
MBR_Widht, nm	mean	129.99	132.07
	st. dev	50.87	56.71
Elongation shape factor	mean	0.66	0.74
	st. dev	0.17	0.18
Circularity	mean	0.72	0.46
	st. dev	0.15	0.16

Based on the visual assessment the difference between NPs-1 laboratory obtained and commercial NPs-2 nanoparticles is clear by noticed. Quantitative analysis shows that although the significant differences in the shape what is easily observed, obtained values of analyzed parameters of NPs-1 and NPs-2 differ considerably less than could be expected and do not allow for unambiguous classification of the analyzed grains of laboratory or commercial ones. In general NPs-2 – commercially available – are bigger those obtained in the laboratory. NPs-2 exhibits higher mean area (by 18%) and MBR_ Height by 13% in respect to NPs-1. Also the standard deviations of those values are higher (especially for the mean area – greater by 20%). Such results suggest that a spread of the grain size is wider for NPs-2 (see Table 2). NPs-2 is more elongated in comparison to NPs obtained by laboratory means. NPs-1 is also more circular then those comerciallycommercially available. Only shape factor of circularity shows a distinct difference in values, and analysis of obtained values confirms that commercial nanograins characterizes more complex perimeter, what is due to the effect of the irregular, jagged border line. The average of nanoparticles smallest dimension (MBR_Height) is 85.2 nm with a standard deviation of 36.43 nm what also indicates that those particles exhibit higher probability of entering nanopores in the Al_2O_3 coatings.

CONCLUSION

The NPs-1 and NPs-2 has the same crystal structure and chemical composition as was confirmed during TEM examination. The results of quantitative analysis obtained from the computer image analysis shows that, the size analysis do not show so significant differences between the compared nanopowders as expected. NPs-2 – commercially available are generally bigger, more elongated, less circular with irregular, jagged border line. Visual comparative analysis showed the NPs-1 and NPs-2 had different quality which greatly affected their ability to form agglomerates, and hence it had magnificent influence on the possibility of introducing the NPs to the nanopores.

РЕЗЮМЕ. Аморфні оксидні шари Al_2O_3 отримано на алюмінієвому сплаві EN AW 5251. Вивчено їх мікроструктуру. У покрив Al_2O_3 вводили два типи неорганічних фулереноподібних (НФ) вольфрамдисульфідних (WS_2) наночастинок (НЧ) методом занурення. Показано відмінність впливу введення НЧ на мікроструктуру Al_2O_3 та проведено електронну мікроскопію покривів. Обробкою зображень мікроструктур та їх аналізом вивчено форму та розмір наночастинок НФ-WS_2. Порівняльний аналіз нанопорошків щодо їх агломерування показав відмінності, які найбільше впливають на здатність їх проникнення в нанопори.

РЕЗЮМЕ. Аморфные оксидные слои Al_2O_3 получены на алюминиевом сплаве EN AW 5251. Изучена их микроструктура. В покрытие Al_2O_3 вводили два типа неорганических фуллереноподобных (НФ) вольфрам дисульфидных (WS_2) наночастиц (НЧ) методом погружения. Показано различие влияния введения НЧ на микроструктуру Al_2O_3 и проведено электронную микроскопию. Обработкой изображений микроструктур и их анализом изучено форму и размер наночастиц НФ-WS_2. Сравнительный анализ нанопорошков касательно их агломерирования показал различия, более всего влияющие на способность их проникновения в нанопоры.

1. *Friction* mechanism of individual multilayered nanoparticles / O. Teveta, P. Von-Huth, R. Popovitz-Biro, R. Rosentsveig, H. D. Wagner, and R. Tenne // Proc. Nation. Acad. Sci. of the USA. – 2011. – **108**, № 50. – P. 19901–19906.
2. *Mechanism* of Action of WS_2 Lubricant Nanoadditives in High-Pressure Contacts / M. Ratoi, V. B. Niste, J. Walker, and J. Zekonyte // Tribol. Lett. – 2013. – **52**, № 1. – P. 81–89.
3. *Influence* of particle agglomeration on the catalytic activity of carbon-supported Pt nanoparticles in CO monolayer oxidation / F. Maillard, S. Schreier, M. Hanzlik, E. R. Savinova, S. Weinkauf, and U. Stimming // Phys. Chemistry Chemical Physics. – 2005. – **7**. – P. 385–393.
4. *Handbook* of Lubrication and Tribology: Theory and Design, 2nd Edition / Ed.: R. W. Bruce. – London; New York: Taylor & Francis Group, 2012. – **2**. – 66 p.

5. *Experimental* Investigation of Particle Size Effect on Agglomeration Behaviors in Gas−Solid Fluidized Beds / J. Wang, Q. Shi, Z. Huang, Y. Gu, L. Musango, and Y. Yang // Ind. Eng. Chem. Res. – 2015. – **54**. – P. 12177−12186.
6. *New* reactor for production of tungsten disulfide hollow onion-like (inorganic fullerene-like) nanoparticles / Y. Feldman, A. Zak, R. Popovitz-Biro, and R. Tenne // Solid State Sci. – 2000. – **2**. – P. 663–672.
7. *Continuous* Production of IF-WS_2 Nanoparticles by a Rotary Process / F. Xu, N. Wang, H. Chang, Y. Xia, and Y. Zhu // Inorganics. – 2014. – **2**. – P. 313–333.
8. *Wolfrom R. L.* The language of particle size // GXP Compliance. – 2011. – **15**, № 2. – P. 10–20.
9. *Escobar J., Arurault L., and Turq V.* Improvement of the tribological behavior of PTFE anodic film composites prepared on 1050 aluminum substrate // Appl. Surf. Sci. – 2012. – **258**, № 20. – P. 8199–8208.
10. *Lu G. Q. and Zhao X. S.* Nanoporous Materials // Sci. and Eng. – London: Imperial College Press., 2004.
11. *Kralchevsky P. A. and Nagayama K.* Capilary forces between colloidal particles // Langmuir. – 1994. – **10**. – P. 23–36.
12. *Nagayama K.* Two-dimentional self-assembly of colloids in thin liquid films // Colloids and Sufraces A. – 1996. – **109**. – P. 363–374.
13. *Hu N-N., Ge S-R., and Fang L.* Tribological properties of nanoporous anodic aluminum oxide template // J. Cent. South Univ. Technol. – 2011. – **18**, № 4. – P. 1004–1008.
14. *Two-step* method for preparation of Al_2O_3/IF–WS_2 nanoparticles composite coating / J. Korzekwa, R. Tenne, W. Skoneczny, and G. Dercz // Phys. Status Solidi A. – 2013. – **210**. – P. 2292–2297.
15. *Tribological* behaviour of Al_2O_3/inorganic fullerene-like WS_2 composite layer sliding against plastic / J. Korzekwa, M. Bara, J. Pietraszek, and P. Pawlus // Int. J. Surf. Sci. and Eng. (In press.)
16. *Russ J. C.* The image processing handbook // CRC. – Florida: Press. Boca Raton, 1994.

Received 07.12.2016